nature human behaviour

ARTICLES

https://doi.org/10.1038/s41562-017-0249-4

Right but not left hemispheric discrimination of faces in infancy

The result section of this version has been edited to correct 1) an error on the degrees of freedom when condition was a factor, 2) inconsistencies between the table and the text. These corrections do not affect the reported significance of the results which were computed with the true values. GDL

Parvaneh Adibpour, Jessica Dubois and Ghislaine Dehaene-Lambertz*

The ontogeny of the functional asymmetries of the human brain is poorly understood. Are they a consequence of differential development based on competition mechanisms, or are they constitutive of the human brain architecture from the start? Using structural magnetic resonance imaging and a face-discrimination electroencephalography paradigm with lateralized presentation of faces, we studied face perception in infants over the first postnatal semester. We showed that the corpus callosum is sufficiently mature to transfer visual information across hemispheres, but the inter-hemispheric transfer time of early visual responses is modulated by callosal fibre myelination. We also revealed that only the right hemisphere shows evidence of face discrimination when presented in the left visual hemifield. This capability improved throughout the first semester with no evidence of discrimination in the left hemisphere. Face-processing lateralization is thus a characteristic of the infant's extra-striate visual cortex, highlighting the differential left–right organization of the human brain already established in infanthood.

The adult human brain is divided into multiple functional regions that are remarkably similar across individuals despite differences in cultural, linguistic or socio-economic background. Even for culturally learned skills, such as reading, similarly localized activations are observed across writing systems and ages of acquisition[1], revealing the weight of structural constraints on functional architecture. Despite a growing body of evidence on the existence of specialized functional modules in the adult brain, the developmental course of such functional specialization is still poorly understood. Hemispheric functional asymmetries represent a radical example of functional specialization, because a priori similar cortical areas end up with different functional specificities.

Here, we aimed to understand the origin of the right-hemispheric advantage for face processing. Two main hypotheses can be proposed. The first hypothesis proposes that structural differences between hemispheres result in a higher efficiency of the right hemisphere to process faces from the start. These structural differences might be determined early on during gestation based on cortical 'protomaps'[2]. They may also be driven or amplified by maturational asymmetries in grey- or white-matter pathways, which would give rise to a transitory advantage in one hemisphere when infants are exposed to frequent and expected stimuli, such as speech and faces[3,4]. In line with this first hypothesis, asymmetries in cortical maturation[5] and in bundle myelination[6,7] have already been reported in the language network during the first semester after birth. The second hypothesis postulates that both hemispheres are equally competent at the onset of development and responses to faces become restricted to the right hemisphere as infants and children enlarge their visual world and learn new visual categories[8]. The organization of the final mosaic of specialized regions in the adult brain is determined through competition possibly weighted by inherent structural connectivity advantages[9]. For example, visual word-specific activation is left lateralized in order to reduce the path length toward the oral language network, resulting in a competition between words and faces to occupy the same territory in the left hemisphere[10]. This idea is supported by evidence of more right-lateralized responses to faces in normal readers compared to dyslexic children[11] and illiterate adults[12]. In both hypotheses, connectivity, maturation and exposure have an influence on the final organization; however, they diverge on the initial organization of the brain. The first proposes initial neural specificities of genetic origin that constrain the processing of the visual environment, whereas the second emphasizes the role of the environment in determining the organization of the brain. This debate is not purely theoretical as plasticity might be reduced in areas committed to specific functions, explaining long-term effects of early sensory deprivation[13] and, more generally, inadequate early stimulation.

Faces are the first and most frequent visual stimulus to which infants are exposed, and face recognition is crucial to establish social bonding. Face perception is hypothesized to rely on both innate biases for orienting one's gaze to face-like stimuli and personal experience in discriminating faces of one's entourage[14–16]. From birth on, neonates discriminate their mother's face from a stranger's initially using predominantly the hairline and outer contour of the head[17,18]. They tolerate only a slight deviation from the frontal view in recognizing the same face[19]. During the first months after birth, they rapidly progress in recognizing novel faces, even when presented in different orientations[20], and perform better for ethnic faces with which they are most familiar[21] and the gender that is most represented around them[22–24].

What are the neural bases of this rapid and efficient learning? Is there already a right-hemisphere advantage to process faces in infants? Electro-encephalography (EEG is the easiest technique to use to study the infant brain. Two evoked-related response (ERP) components, the N290 and P400 (which correspond to an electric negativity (N) around 290 ms and a positivity (P) around 400 ms), have been reported to be modulated by face perception[25–28] and face discrimination[24,29–31]. Although a larger right response has been reported in some studies[26,32], these components are commonly measured bilaterally. Recently, 4–6-month-old infants were shown to recognize faces in different orientations in natural scenes, and the face-selective responses highlighted by a frequency-tagging approach appeared to be strongly right lateralized[33], in agreement with the hemispheric asymmetries described in adults using the same method[34].

Cognitive Neuroimaging Unit, CEA DRF/I2BM, INSERM, NeuroSpin Center, Université Paris-Sud, Université Paris-Saclay, Gif-sur-Yvette, France.
e-mail: ghislaine.dehaene@cea.fr

Near-infrared spectroscopy (NIRS) studies confirm an early right-hemispheric superiority. Using a recording patch over the temporal areas in 5–8-month-old infants, previous studies showed a bilateral response to canonical upright faces relative to a baseline of vegetable pictures[35–37], but a right-hemispheric advantage emerged when canonical versus scrambled faces[35] and upright versus inverted faces[37] were contrasted. The response in the right hemisphere progressively enlarged during the third trimester of life, notably for other views of a face[38]. Positron emission tomography (PET) and functional magnetic resonance imaging (fMRI) studies in young children are surprisingly less conclusive. Responses to faces have been localized to the fusiform regions in infants[39,40], but they might be less specific to such stimuli than later in life, as these regions were similarly activated by faces and objects in 3–8-month-old infants compared to adults[40]. The reported fusiform activations were either not lateralized[40] or weakly right lateralized[39]. Note that in NIRS studies, measurements from a large temporal recording patch were merged. This may increase the sensitivity to small but consistent differences in each voxel from the ventral temporal areas but may also sum up activity from different regions involved in face perception—that is, the fusiform gyrus, the occipital face area and the posterior superior temporal region—that were reported but not merged for analyses in the fMRI and PET studies. Face-specific activations measured with fMRI in the ventral visual areas remain weak over a long period. Hardly observed in young children at 5–8 years of age[41] (but see ref. [42]), face-selective responses in the fusiform gyrus progressively enlarge throughout childhood, with a stronger right lateralization in adults than in children[43–45]. A longer period of cortical microstructural changes in the posterior fusiform gyrus than in neighbouring areas might support this long functional development[46].

Another way to establish each hemisphere's specificities is to exploit visual hemifield presentation: owing to the organization of the visual pathways, only the contralateral hemisphere is informed to the stimulus until inter-hemispheric transfer occurs. In adults, the reaction times for recognizing faces are faster when presented in the left hemifield (right hemisphere) than in the right hemifield wheres opposite results are obtained for word reading[47]. A left-hemifield alexia reported in a patient with a lesion of the splenium[48] and the requirement of a left-hemifield presentation to encode face identity across different orientations[49] are some of the examples that establish the superiority of one or the other hemisphere in adults and the need to transfer information to the specialized hemisphere for correct processing.

In infants, a left-hemifield (that is, a right-hemisphere) superiority was observed in three-month-olds, who oriented faster to familiar faces presented in the left hemifield than in the right[50,51]. A robust left-hemifield superiority was also reported when the two faces were differing in eye size and eye orientation but a reverse effect (~~left~~-hemifield–~~right~~ hemisphere advantage) was observed when differing for by their eye shape in 4–10-month-old infants[52]. However, behavioural experiments cannot disentangle the following hypotheses: (1) both hemispheres perform the task but the left hemisphere is slower than the right; or (2) only the right hemisphere performs the task, revealing a radical dissociation as reported in adults.

Reverse left and right

Furthermore, if both hemispheres have different competencies, what is the role of the corpus callosum in amplifying or reducing these differences? This large pathway is completed during gestation[53], but its myelination continues until adolescence. With regards to the splenium fibres that connect visual regions, their myelination begins after the third postnatal month and rapidly progresses until the end of the first year[54,56] and possibly later on[56]. We therefore wondered whether this rapid maturation has a role in the development of left–right functional asymmetries allowing the most competent hemisphere to inhibit the other[57] or whether the callosal fibres only follow the maturational development of the connected visual areas.

To explore the question of inter-hemispheric transfer, a conditional learning paradigm was previously used in which infants learned to orient to an upper toy for one image and to a lower toy for another image. The images were first presented in one hemifield, and it was analysed whether the number of trials to reach the learning criterion was reduced for the same images secondarily presented in the other hemifield, thus revealing the transfer of learning from one hemisphere to the other. A transfer was observed at 6 months of age when a face and a scrambled face were presented[58] but no inter-hemispheric transfer was observed before 24 months of age when two faces were used[51,52,59]. Therefore, reconsidering the first study[58], it has been hypothesized that face categorization was probably conveyed through subcortical pathways to both hemispheres and that face identity encoding required the corpus callosum, which was not fully functional before the second year of life. By contrast, it has been shown that neonates were able to transfer tactile and haptic information from one hand to the other[60]. The discrepancy between these results may be related to a different experimental sensitivity, but are more likely to be related to the fibres connecting perirolandic sensory regions that are consistently more mature than visual splenium fibres from gestation onwards[61].

We therefore aimed to reconsider these questions because of the opportunities offered by coupling structural and functional brain imaging techniques. We used diffusion MRI and high-density (128 channels) EEG in a group of 40 infants aged between 1 and 6 months; 13 of whom completed both diffusion MRI and EEG tests. We first assessed the influence of connectivity on the infant's visual responses by correlating the speed of visual ERPs with diffusion tensor imaging (DTI) measurements of white-matter maturation obtained in the same infants. DTI can be used to follow white-matter myelination throughout infancy owing to its sensitivity to water molecule diffusion[6,62–65]. Water diffusion becomes preferentially channeled along axons with the progressive myelination of the fibres, resulting in a decrease in transverse diffusivity. In parallel, myelination accelerates the conduction of neural responses, which can be captured on the scalp through decreases in the latencies of the ERP components. For central stimuli, for instance, the latency of the first visual evoked component (P1) shifts from around 300 ms at birth to about 120 ms at 12 weeks of age[66]. We have previously related this acceleration to the myelination of the optic radiation and, notably, to a decrease in transverse diffusivity[6]. Here, we first compared the P1 latency for central and lateralized stimuli, and correlated the speed of the P1 response appearing on the contralateral hemisphere to the transverse diffusivity of the optic radiation. We also measured the inter-hemispheric transfer time (IHTT) as the difference between the contra- and ipsilateral P1 and correlated its related speed with the transverse diffusivity in the splenium fibres that connect the visual areas. In adults, a shorter IHTT has been shown to correlate with lower mean diffusivity[67], higher fractional anisotropy[68] and higher axon diameter[69] in the posterior part of the corpus callosum.

Second, we evaluated each hemisphere's competency in discriminating lateralized faces. Are both hemispheres or is only the right hemisphere reacting to a new face? How is information on face identity exchanged between hemispheres? Therefore, we exposed infants to two streams of faces in the left and right hemifield. One face was assigned to one hemifield and was presented frequently (standard image). Occasionally deviant faces, defined as either a new face (new-deviant image) or the standard face of the other side (known-deviant image), were presented. The new-deviant condition was used to separately study each hemisphere's response to change and therefore to compare their efficiency. The known-deviant condition was used to study the functional efficiency of the corpus callosum at this age. We hypothesized that if the corpus callosum is already efficient, the ipsilateral face (known-deviant image) should be considered as familiar as the contralateral face (standard image), whereas if there is no

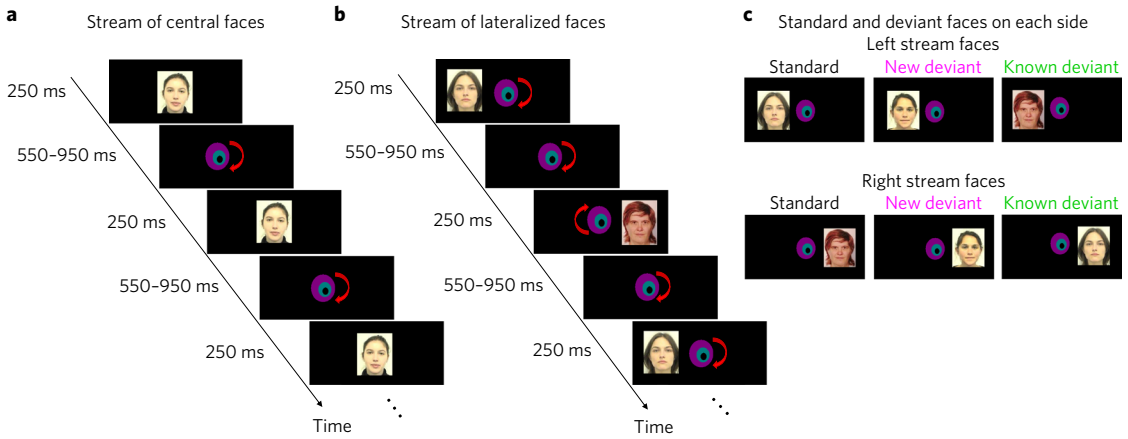

Fig. 1 | EEG experimental paradigms. a, Centralized presentation: a stream of female (or male) face images was presented at the centre of the screen. Each face was presented during 250 ms, separated by a random interval of 550–950 ms during which a rotating and coloured bull's eye was presented at the centre of the screen. **b**, Lateralized presentation: two streams of face images were presented in the left and right visual hemifields in an alternating fashion. The coloured bull's eye was always rotating at the centre of the screen to attract the infants' gaze towards the centre of the screen and to avoid saccades to the periphery. In each block of the experimental design, one face image was attributed to each side and was presented for 250 ms followed by a post-stimulus random interval of 550–950 ms. Each block consisted of only female or only male images. **c**, The different conditions of the lateralized paradigm: for each block, one standard face was attributed to one side and presented in approximately 80% of trials. In around 10% of trials, known-deviant faces corresponded to the standard faces on the incorrect side whereas new deviant faces were rare faces with no attributed side (around 10% of trials). For copyright reasons, the right standard face is different from the one presented in the experiment.

inter-hemispheric transfer, it should be considered as novel as the new-deviant face.

Results

An efficient inter-hemispheric transfer of early visual responses in infants. *ERPs responses.* Brain visual responses to faces were recorded with a high-density EEG system (128 channels) in infants aged between 5.6 and 23.6 weeks. Twenty-three infants were tested with central faces (Fig. 1). The P1 latency measured over mid-occipital areas decreased with age from 185 to 121 ms ($R^2 = 0.41$, $P < 0.001$ in 23 infants; Fig. 2a,c) and reached a plateau around 12 weeks of age (Fig. 2c). This decrease in P1 latency was better fitted with a third degree polynomial ($R^2 = 0.72$, $P < 0.001$) than with a linear model (Akaike's information criterion[70] (AIC) polynomial model = 179; AIC linear model = 189).

Lateralized faces were used in 40 infants (including the 23 infants mentioned above). An initial response in the contralateral hemisphere was identified followed by a response in the ipsilateral

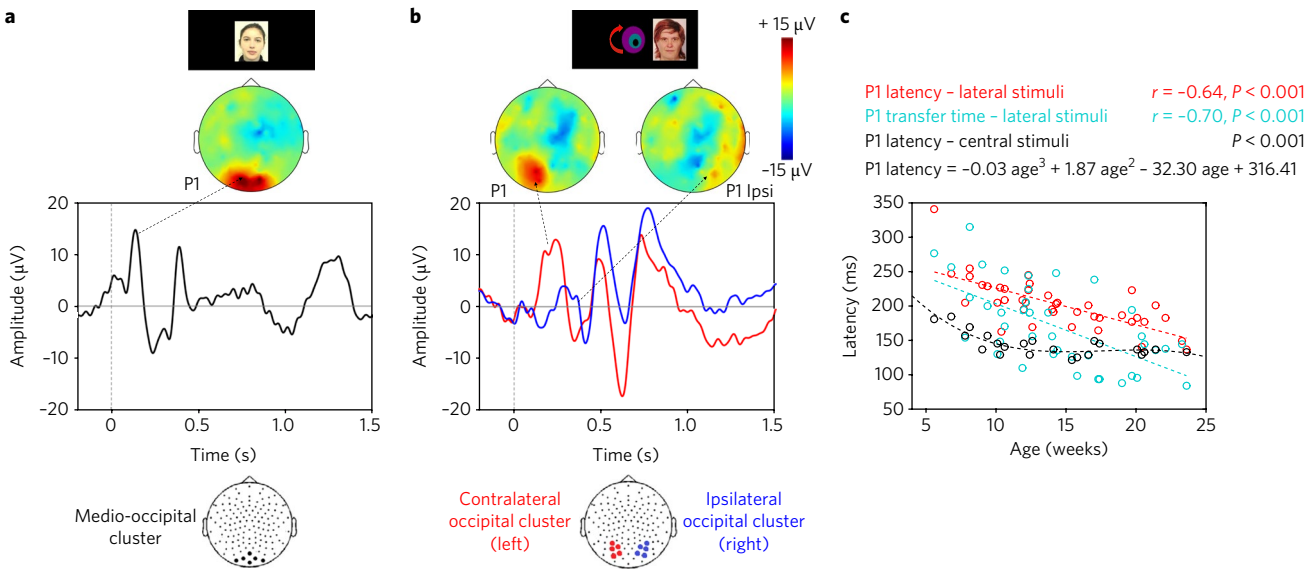

Fig. 2 | P1 component. a, Voltage-time course in response to central stimuli averaged over a cluster of electrodes covering the mid-occipital region in one infant (21 weeks old). Time zero marks the onset of the face stimuli. **b**, Responses to faces presented in the right hemifield averaged across the left and right occipital clusters of electrodes (red and blue curves, respectively) for the same infant. The contralateral P1 appears over the left hemisphere and then propagates towards the ipsilateral hemisphere. **c**, Relation between P1 latencies and infants' age: P1 for central stimuli (black curve, 23 infants), contralateral P1 for lateralized stimuli (red curve and text, 40 infants), and inter-hemispheric transfer-time (cyan curve and text, 40 infants). P1 latencies were faster for central than for lateralized stimuli and reached a plateau at 12 weeks of age, whereas the decrease was linear for the contralateral P1 and the inter-hemispheric transfer times.

hemisphere (Fig. 2b). The P1 latency for contralateral responses to lateralized faces was slower than the responses to central faces ($t_{1,22}=9.3$, $P=0.004$) and linearly decreased with age (from 341 to 137 ms, $R^2=0.51$, $P<0.001$ in 40 infants; Fig. 2c). The IHTT similarly decreased from 315 to 84 ms ($R^2=0.39$, $P<0.001$: Fig. 2c). The age-related slopes did not differ between the contralateral P1 latency and IHTT ($t_{1,39}=1.5$, $P>0.1$). Finally, P1 latencies and IHTT were similar for faces in the left and right hemifield (P1: $t_{1,39}<1$, $P>0.1$; IHTT: $t_{1,39}=-1.5$, $P>0.1$).

DTI measurements. The maturation of the optic radiations and commissural fibres was studied in 22 infants imaged with diffusion MRI and compared to the equivalent tracts in the auditory domain to control for general vs domain-specific maturation. We dissected the optic (OR) and acoustic radiations, the visual (vCC) and auditory callosal fibres (aCC) with probabilistic tractography (Fig. 3a). For all tracts, DTI transverse diffusivity significantly decreased with age (Fig. 3b, $-0.87<r<-0.68$, $P<0.001$). Using partial correlations to remove global effects of the age of the infants (Table 1, Fig. 3d), we observed significantly correlated maturational patterns for the microstructural properties of optic radiations and visual callosal fibres ($r_{(\mathrm{OR\text{–}vCC}\mid \mathrm{age})}=0.78$, $P<0.001$) and for the visual and auditory callosal fibres ($r_{(\mathrm{vCC\text{–}aCC}\mid \mathrm{age})}=0.74$, $P<0.001$). These results suggest that bundles belonging to the visual network mature in synchrony similar to the callosal fibres connecting visual and auditory regions in the splenium. Finally, transverse diffusivity was lower in the left relative to the right hemisphere in both optic radiations ($t_{21}=-5.3$, $P<0.001$) and auditory radiations ($t_{21}=-5.1$, $P=0.001$), suggesting an advanced maturation in the left hemisphere tracts.

In a subgroup of 13 infants for whom both the ERP lateralized paradigm and diffusion MRI had been acquired, we investigated whether the conduction speed of visual evoked responses (that is distance divided by latency, see Methods) was related to the maturational properties of the underlying pathways. Using partial correlations

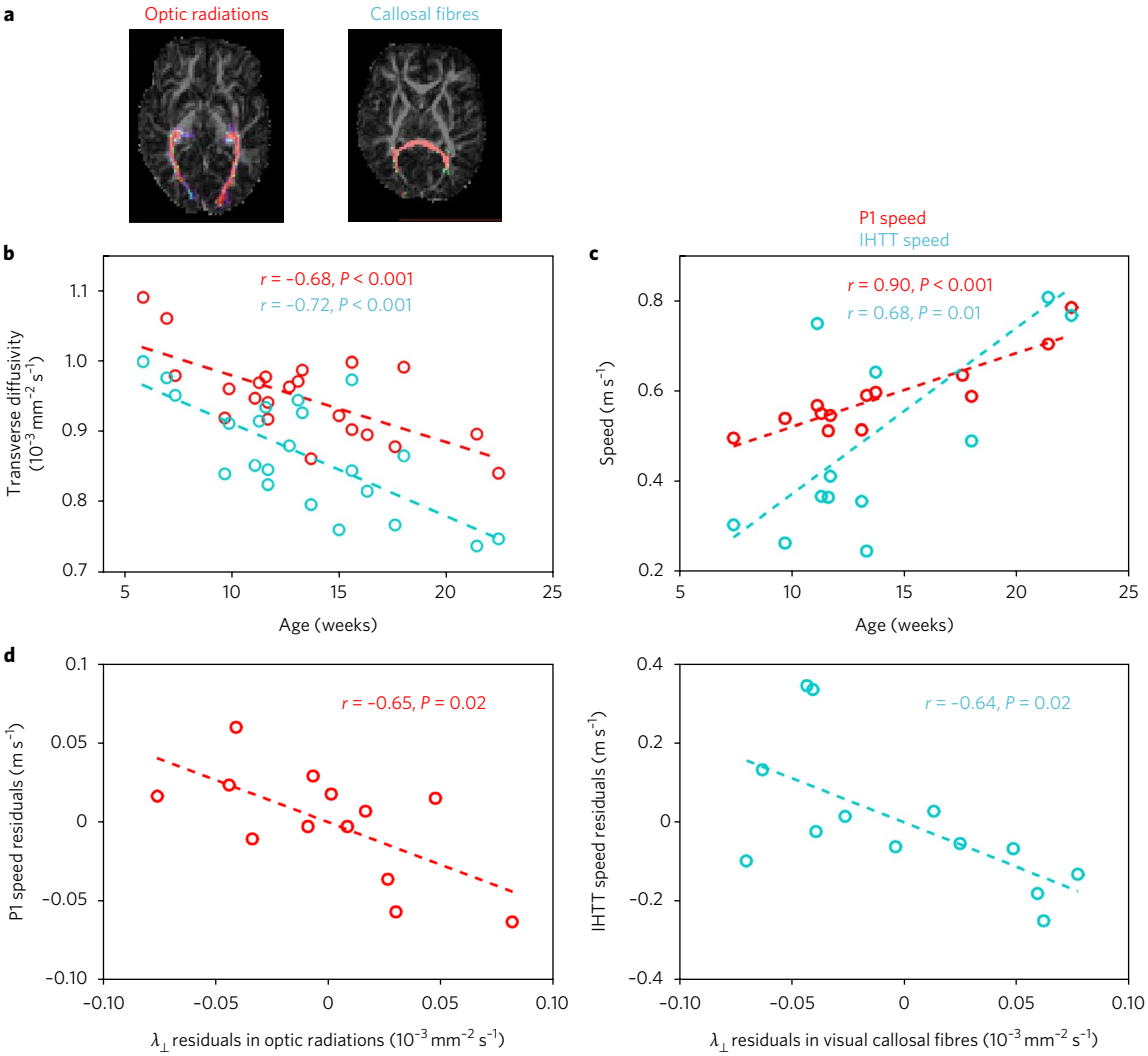

Fig. 3 | Structure–function relationships. a, Reconstructed bundles of the visual network in one infant (12 weeks old): optic radiations, extending from the lateral geniculate nucleus to occipital regions (left), and callosal fibres connecting the occipital regions and passing through the splenium (right). **b**, Age-related decrease of transverse diffusivity in optic radiations (red) and visual callosal fibres (blue) in the 22 infants with MRI data. **c**, Age-related increase in response speeds (speed is approximately equal to anatomical distance divided by latency) corresponding to P1 (red) and IHTT (cyan) responses in the 13 infants with both EEG and MRI data. **d**, Relationships between the response speed and transverse diffusivity ($\lambda_\perp$) in the corresponding tract for the 13 infants with EEG and MRI data. Partial correlations were performed to demonstrate that speeds are related to diffusivities, independently of age. To visualize such relationships, we here show the residuals once the effect of age was removed, for P1 (left) and IHTT (right) speeds in relation to $\lambda_\perp$ in the optic radiations (left) and visual callosal fibres (right). *r* and *P* values correspond to partial correlations reported in the text and Table 1.

Table 1 | Evaluation of structural maturation with DTI

Maturational relationships across bundles				Structure function relationships		
	vCC	AR	aCC		Speed P1	Speed IHTT
OR	$r=0.78$, $P<0.001$	$r=0.63$, $P=0.004$	$r=0.55$, $P=0.014$	OR	$r=-0.65$, $P=0.021$	
vCC		$r=0.35$, $P>0.1$	$r=0.74$, $P<0.001$	vCC		$r=-0.64$, $P=0.025$
AR			$r=0.42$, $P=0.069$	AR	$r=-0.45$, $P>0.1$	
aCC				aCC		$r=-0.65$, $P=0.021$

Left, partial correlations were computed for transverse diffusivity in the different pairs of bundles, while controlling for the age of the infants. Optic and acoustic radiations, visual and auditory callosal fibres are abbreviated by OR and AR, vCC and aCC, respectively. Right, partial correlations were computed between the speed of P1 or IHTT and transverse diffusivity in similar bundles of the visual and auditory networks, while controlling for age. *P* values are corrected for the number of comparisons by false-discovery rate (FDR).

to account for the age of the infants (Table 1), we observed that the speed of the contralateral P1 was related to the maturation of optic radiations ($r_{(\text{Speed}_{P1}-\text{OR}|\text{age})}=-0.65$, $P=0.021$; Fig. 3b), whereas the speed of inter-hemispheric transfer was related to the maturation of visual and auditory callosal fibres ($r_{\text{Speed}_{\text{IHTT}}-\text{vCC}|\text{age})}=-0.64$, $P=0.025$; Fig. 3c; $r_{\text{Speed}_{\text{IHTT}}-\text{aCC}|\text{age})}=-0.65$, $P=0.021$).

Together, these results reveal that the inter-hemispheric transfer of early visual responses is already efficient during infancy and is strongly related to the maturation of the underlying callosal fibres.

An efficient discrimination of left-hemifield faces. In the second step of this study, we evaluated whether infants were able to discriminate faces that were presented either in the left or right hemifields (Fig. 1c). Figure 4 shows the grand average ERP on the ipsi- and contralateral clusters for each stimulated visual hemifield, all conditions merged (standard, new-deviant and known-deviant faces). We focused our ERP analyses on the P1, to examine the effects of low-level features, and on the N290 and P400 components, which are the classical components related to face perception in the infant literature[25] (Figs. 4–6 and Supplementary Fig. 1). In each of the 40 infants tested with the lateralized paradigm, we averaged the voltage over three 100-ms time windows (P1: 150–250 ms; N290: 300–400 ms; P400: 450–550 ms) and over symmetrical left and right clusters of 10-electrodes in the occipito-temporal regions (see Methods for the choice of temporal windows and electrodes). We entered these values into separate analyses of variance (ANOVAs) with condition (three levels), hemifield (two levels) and cluster (two levels) as within-subject factors. For the P1, the ANOVA revealed a significant interaction of hemifield by cluster ($F_{1,39}=26.5$, $P<0.001$), because, as expected for a lateralized stimulation, the contralateral response was larger than the ipsilateral response (for each hemifield, $P<0.001$). A modest trend for an interaction of condition by cluster was also present ($F_{1,39}=2.6$, $P=0.08$). For the N290, there was a main effect of condition ($F_{1,39}=3.4$, $P=0.039$), a marginally significant effect of cluster ($F_{2,78}=3.6$, $P=0.065$), a significant interaction hemifield by cluster ($F_{2,78}=15.1$, $P<0.001$) and a marginally significant interaction between condition and cluster ($F_{2,78}=2.7$, $P=0.074$). For the P400, only a main effect for hemifield was observed ($F_{1,39}=5.1$, $P=0.030$). We then analysed each hemifield separately.

Responses to left-hemifield faces. For the P1, there was no effect of condition on the contralateral ($F_{2,78}=2.4$, $P>0.1$) and ipsilateral ($F_{2,78}<1$) hemisphere. For the N290, an effect of condition was observed across the contralateral right cluster ($F_{2,78}=4.2$, $P_{fdr}=0.016$) but not across the ipsilateral left cluster ($F_{2,78}<1$). Post hoc Students's *t*-test analyses for paired conditions indicated that the N290 amplitude was larger (that is, more negative) for new-deviant faces than for standard and known-deviant faces (respectively: $t_{1,39}=-2.2$, $P=0.031$; $t_{1,39}=-2.7$, $P=0.014$) (Figs. 5a and 6a and Table 2), whereas no difference was detected between standard and known-deviant faces ($t_{1,39}<1$). Therefore, infants discriminated faces presented in their left hemifield, whereas standard faces from the other side (right hemifield) did not elicit a novelty response, demonstrating that face information had been transferred between hemispheres. The N290 amplitude difference between new and standard faces became larger with age ($r=-0.38$, $P=0.047$; Fig. 6c) due to an increase of the N290 absolute amplitude in response to new-deviant faces. No age effect was observed for the difference between new- and known-deviant faces ($r=-0.16$, $P>0.1$, Fig. 6c).

The same pattern was seen for the P400. An effect of condition was observed for the contralateral right cluster ($F_{2,78}=3.18$, $P_{fdr}=0.047$) but not for the ipsilateral left cluster ($F_{2,78}<1$). The P400 was significantly weaker for new faces relative to standard faces ($t_{1,39}=-2.3$, $P=0.042$) and known-deviant faces ($t_{1,39}=-2.7$, $P=0.029$), whereas responses to standard and known-deviant faces did not differ ($t_{1,39}<1$) (Figs. 5a and 6a). The difference between new and standard faces tended to become larger with age despite not being robust to multiple comparison corrections ($r=-0.26$, $P>0.1$; Fig. 6c). No age effect was observed for the difference between new- and known-deviant faces ($r=0.16$, $P>0.1$; Fig. 6c).

Responses to right-hemifield faces. There was no significant effect of condition for the P1, N290 and P400 responses, either in the contralateral left or in the ipsilateral right clusters (Figs. 5b and 6b and Table 2). Because we did not anticipate this result, we looked for putatively delayed effects. By visually inspecting the time-series, we selected two later time windows (t_1: 750–850 ms; t_2: 1,050–1,150 ms). Again no effect of condition was found (for the contralateral left cluster: t_1: $F_{1,39}=1.6$, $P>0.1$; t_2: $F_{1,39}=1.7$; $P>0.1$; for the ipsilateral right cluster: t_1: $F_{1,39}<1$; t_2: $F_{1,39}<1$), although new-deviant faces tended to evoke more positive responses than standard faces in the contralateral left cluster (t_1: $t_{1,39}=1.8$, $P=0.071$; t_2: $t_{1,39}=1.9$, $P=0.065$) but not the ipsilateral right cluster ($t_{1,39}<1$, for both t_1 and t_2). Responses to known-deviant faces did not differ for the two other conditions ($P>0.1$ for t_1 and t_2 for both contra- and ipsilateral clusters). Therefore, no reliable difference between conditions was detected in the contra- and ipsilateral hemispheres, revealing that infants were not able to discriminate faces presented in their right hemifield either in the left or right hemisphere.

Finally, we studied whether the responses to standard faces presented in the right and left hemifield were different. The amplitudes of the P1, N290 and P400 were similar for the left and right hemifield, for the ipsi- and contralateral clusters (*P*s > 0.1), confirming not only that both hemispheres were processing the stimuli, but also that responses to left standard faces were not reduced relatively to right standard faces.

Discussion

By combining structural and functional measurements using multimodal imaging, we uncovered several aspects of visual development in human infants. We first confirmed the interdependency between DTI measurements of white-matter maturation and the speed of the neural responses, not only at the level of projection tracts, such as the optical radiations, but also at the level of cortico-cortical tracts, such as the corpus callosum. In particular, the myelination of the splenium fibres supports the progressive acceleration of information transfer between hemispheres during the first postnatal semester. Second, we showed that the right hemisphere, but not the left, discriminates faces presented in the contralateral hemifield. The

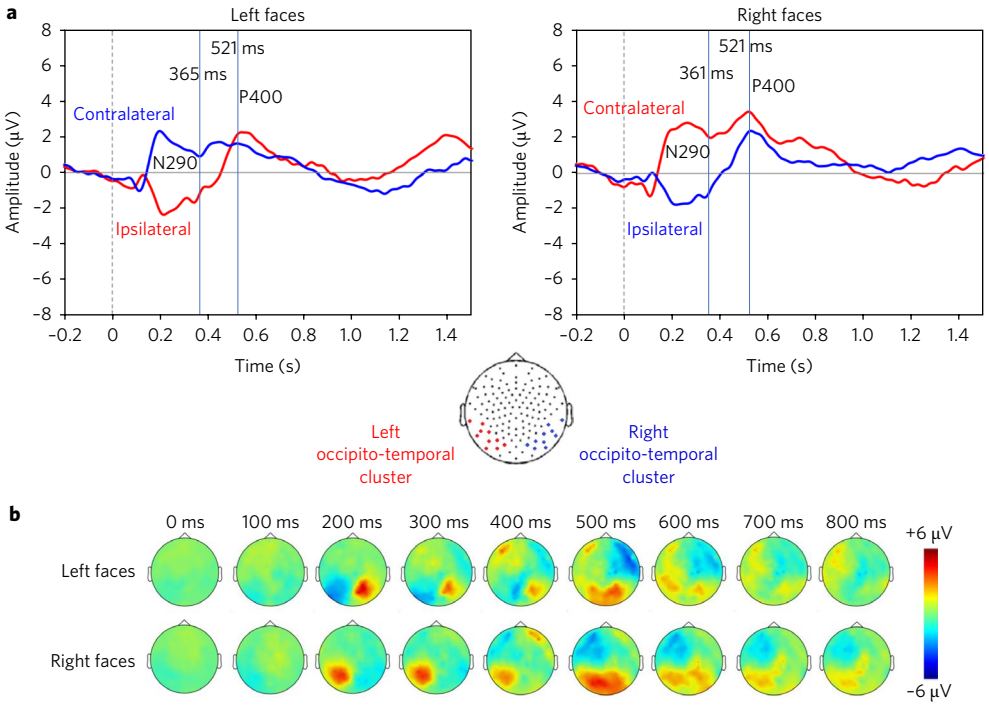

Fig. 4 | Grand averages according to the visual hemifields. a, Grand averages of the 40 infants were computed over the left (red line) and right (blue line) occipito-temporal clusters presented below the plots, for faces presented in the left and right visual hemifields. The peaks of the N290 (365 and 361 ms) and P400 (521 ms) are indicated on the plots. **b**, Two-dimensional voltage topographies in response to left and right faces. The N290 interrupts the positivity on the contralateral cluster and the ascending slope on the ipsilateral cluster. We considered the positivity following the N290 as the P400. Latencies are delayed relative to what is reported for central faces.

response to a new face enlarged and accelerated with age only in the right hemisphere, revealing an improvement in the processing ability of the right hemisphere, whereas the left hemisphere remained unresponsive to face differences. Third, new faces presented in the right hemifield did not evoke any discriminative responses in the left or in the 'competent' right hemisphere, highlighting the still poorly functional inter-hemispheric transfer at this age. Finally, we observed no evidence for an inhibitory role of the corpus callosum on the left responses, because the P1 latencies, the IHTT and the N290 and P400 amplitudes for standard faces did not differ for left- and right-hemifield presentations in either hemisphere.

First, we asked whether fibre-specific microstructural maturation correlates with the acceleration of evoked responses. Age-dependent acceleration of the P1 response has been repeatedly reported for central visual stimuli[6,66,71], reflecting the increasing efficiency of the visual pathway from the retina and lateral geniculate nucleus to the visual cortices. Here, lateralized stimuli evoked delayed P1 responses relative to central stimuli, probably because of the micro-architectural differences between the fovea composed of very dense cones and the peripheral retina primarily containing rods[72,73]. P1 acceleration persisted after 12 weeks of age for lateralized stimuli, whereas the adult latency was already reached for central stimuli at this age. The speed of the early visual responses for lateralized stimuli was related to the transverse diffusivity in the optic radiation independent of age, as we have previously demonstrated for central stimuli[6]. Therefore, myelination of the optic fibres is one of the major factors improving visual efficiency during the first semester of postnatal life beyond the maturation of the peripheral paths and of V1.

The correlation between the structural and functional measurements of development was also seen for callosal connections and the speed of inter-hemispheric transfer. We measured IHTT in infants and related its speed increase to the maturation of splenium callosal fibres connecting occipital regions. IHTT shortened from 300 ms in the youngest to 84 ms in the oldest infants. This delay is notwithstanding far longer than in adults: 7–13 ms in response to checkerboards[74], 15 ms in response to white squares[68], 30 ms in in response to faces[75], but is in the expected range for thin unmyelinated callosal fibres for which conduction delays are between 100 and 300 ms[76]. The maturation of visual callosal fibres was significantly correlated with the maturation in the optic but not the auditory radiations, indicating domain-related rather than a general maturation. Therefore, diffusion MRI might be a practical tool for following the efficiency of white-matter pathways during development and to reveal neural connectivity through correlated maturation not only in normal but also in pathological populations.

Next, we focused on our main goal and studied the ability of each hemisphere to process faces by using two streams of faces in the left and right visual hemifields. We are confident that almost all faces were seen in a lateralized hemifield based on several arguments. Firstly, at the experiment level, the short duration of face presentations (250 ms) was below the time delay for a saccadic eye movement at this age, which is about 400 ms in 4-month-old infants[77]. The randomized delay between faces prevented infants from predicting the exact stimulus onset and orienting their gaze to the corresponding hemifield. We further inspected the video recordings of the infants' behaviour during the experiment to verify that they were continuously centred with respect to the screen and that they did not shift their gaze toward the side of the screen. Secondly, the identification of contralateral P1 responses to left and right faces confirmed that infants were focused on the central distractor at the onset of the lateralized stimulation (see Figs. 2 and 4). This response was followed by ipsilateral responses, and the significant correlation between the IHTT and the maturation of the splenium callosal fibres validates that we were measuring a genuine transfer of information between hemispheres. Finally, the similar succession of components

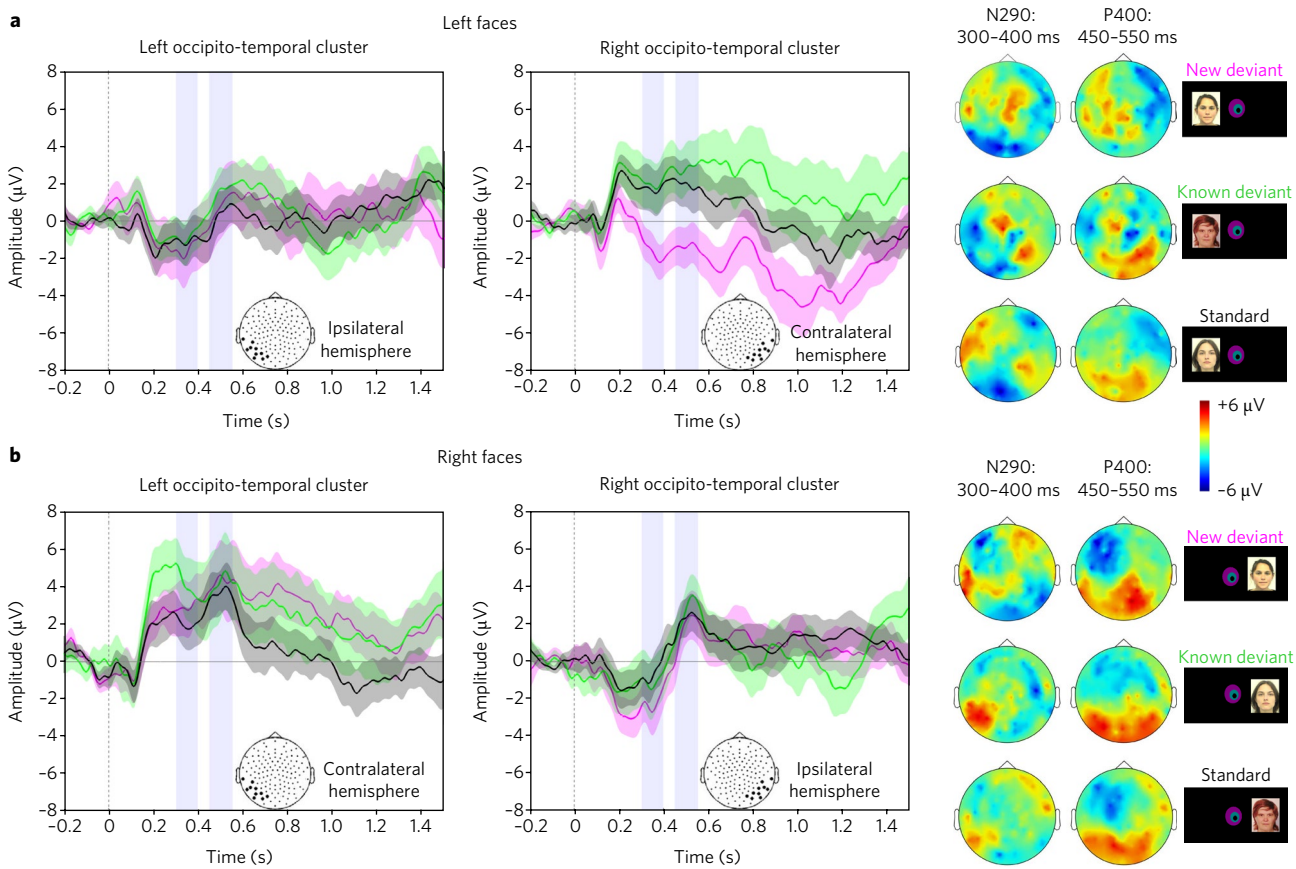

Fig. 5 | Grand averages according to the face conditions. a,**b**, Grand averages of the 40 infants were computed over the left and right occipito-temporal clusters (left and right plots, respectively) for the new-deviant, known-deviant and standard faces presented in the left (**a**) and right (**b**) visual hemifields. Shaded regions around ERPs represent standard error of the mean. Voltage topographies (right column) were averaged over the 300–400 ms and 450–550 ms time windows (shaded in light blue in the time plots) corresponding to the N290 and P400, respectively (voltage topographies along the whole trial are presented in Supplementary Information). There is a clear discrimination of new faces relative to the standard and known-deviant faces for the left-hemifield faces over the contralateral right cluster, whereas no difference between conditions was observed for the right-hemifield faces.

(P1, N290 and P400; Fig. 4) observed for each hemisphere contralateral to the stimulation confirms that each hemisphere was perceiving and processing the contralateral face. Taken together, these arguments support the reliability of our experimental paradigm to test each hemisphere separately in infants.

With this paradigm using lateralized stimuli, we were able to uncover striking differences between the capabilities of the left and right hemisphere. We recorded discrimination responses only in the right hemisphere for new faces presented in the contralateral left hemifield, revealing, contrary to expectations, a surprisingly incompetent left hemisphere. If any evidence of face-discrimination capacity for the left hemisphere existed in this task, it was a delayed, weak and hardly significant response around 750–850 ms and 1,050–1,150 ms after the stimulus; this is in contrast to the earlier and robust N290 and P400 responses in the right hemisphere. It might be possible that the discrimination between our face images was done on low-level cues. However, if this was the case, we should have expected an early difference at the level of the P1 as has previously been shown in adults[78]. This was indeed not the case (that is, no effect of condition at the level of the P1), but further studies might verify this point by using scrambled images as controls as has previously been used[33].

In adults, the left visual hemifield superiority for faces is related to asymmetrical activation of the right–left fusiform face area for face recognition[79]. In infants, this hemispheric difference was asserted previously on the basis of behavioural studies in which the latency of gaze orientation toward faces presented in the left and right visual hemifield was measured[50,51]: four-month-old infants oriented faster to their mother's face than to a stranger's presented in the left hemifield. Furthermore, the same infants oriented faster toward their mother's face presented in the left rather than their mother's face presented in the right hemifield. In a second task, the infants had to associate the position of a rewarding toy (above or under the screen) with the identity of a face (mother or stranger) presented within the right or left hemifield. They succeeded only when the faces were presented in the left hemifield and therefore processed by the contralateral right hemisphere (that is, 72% compared to 17% of infants reached the learning criterion for left- compared to right-hemifield faces; percentages computed from table 4 in ref. [3]). Our results confirm that infant's orienting failures for right-hemifield faces in this study were related to a genuine difficulty in discriminating the two faces in that hemifield rather than to subsequent difficulties in associating each face with the spatial position of the reward.

In NIRS studies, a right hemispheric superiority was robustly observed when configural perception was tested in 5–8-month-olds (that is, upright versus inverted faces[37] and canonical versus scrambled faces[35]) with a progressive development of a response for other views of the face during the second semester of infancy[38]. Similarly, a strong right hemisphere advantage was reported at 4–6 months of age when faces with different sizes and in different viewpoints were presented among other visual categories in a fast presentation

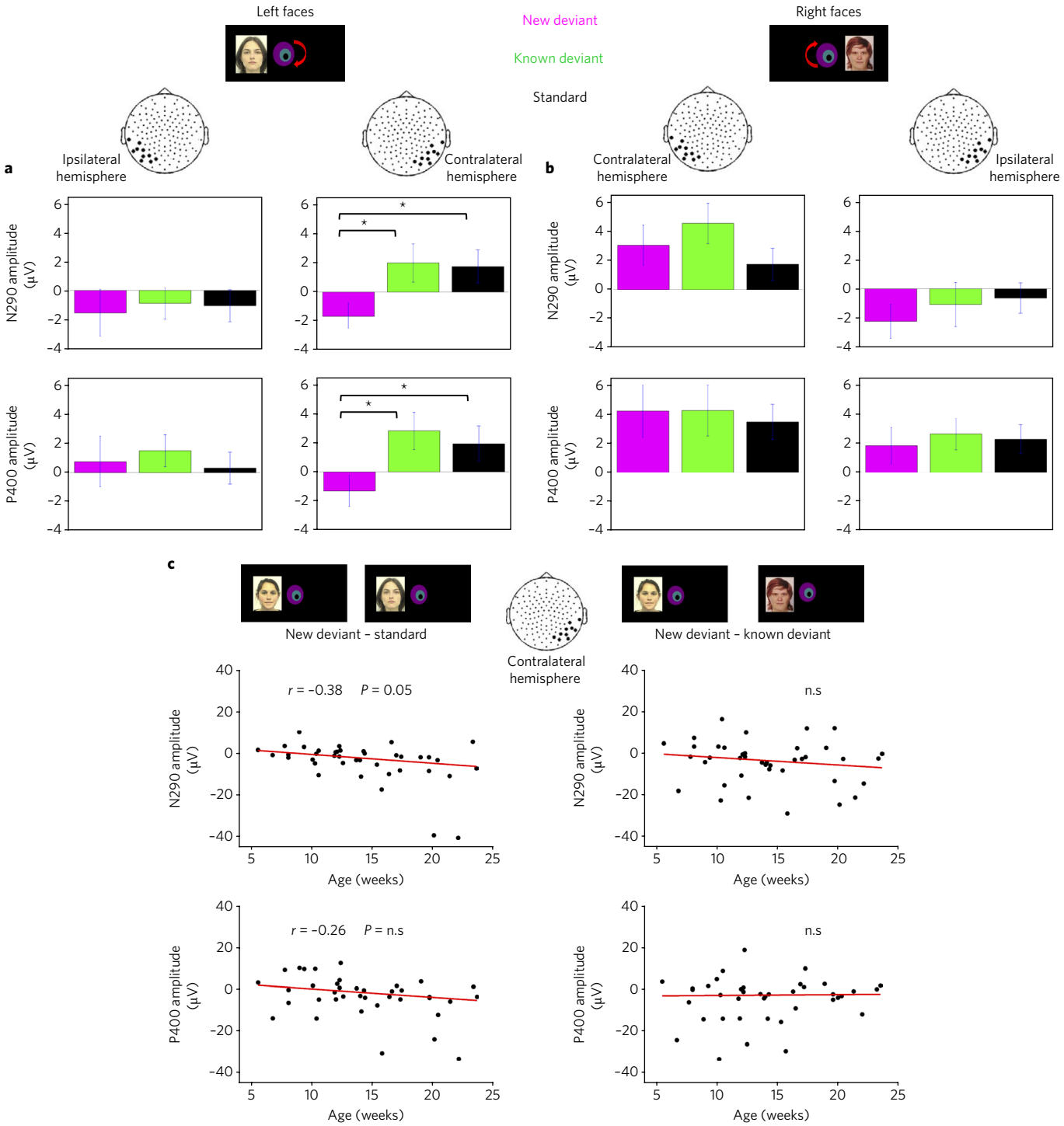

Fig. 6 | Comparison of N290 and P400 components across face conditions. a,**b**, N290 (top row) and P400 (bottom row) amplitudes for faces presented in the left (**a**) and right (**b**) hemifield averaged over the left and right clusters (left and right plots, respectively) in the different face conditions (new-deviant faces in pink, known-deviant faces in green, standard faces in black). The error bars represent the standard error of the mean across the 40 individuals. The asterisks indicate significant differences between conditions after FDR correction for multiple comparisons ($P < 0.05$). **c**, The differences between conditions for left-hemifield faces averaged over the right cluster are plotted as a function of age. There was an increase in the discrimination ability for new-deviant versus standard faces (a significant decrease in N290 amplitude and a non-significant trend for P400 in the left plots) but not versus know-deviant faces (right plots; NS, not significant ($P > 0.1$)).

paradigm. These results suggest that face categorization mainly relies on the right hemisphere from the first months of life onwards. However, discrimination between different faces measured with NIRS induced bilateral responses in 7–8-month-olds[36,80,81]. Here, our paradigm with rapid presentation of faces and divided attention between the two hemifields may have amplified the differences in the face-processing abilities of the left and right hemisphere much in the same way dichotic presentation reveals the superiority of the left hemisphere for speech. The left hemisphere has been shown to be sensitive to facial features[52] that may require a foveal analysis

Table 2 | Comparison of P1, N290 and P400 responses for the different face conditions

	Left occipito-temporal cluster	Right occipito-temporal cluster
Left faces		
P1	$F=0.2$, $P>0.1$	$F=2.4$, $P=0.101$
N290	$F=0.1$, $P>0.1$	$F=5.1$, $P=0.016$ New versus standard: $t=-2.7$, $P=0.014$ Known versus standard: $t=0.2$, $P>0.1$ New versus known: $t=-2.7$, $P=0.014$
P400	$F=0.2$, $P>0.1$	$F=3.9$, $P=0.047$ New versus standard: $t=-2.3$, $P=0.042$ Known versus standard: $t=0.5$, $P>0.1$ New versus known: $t=-2.7$, $P=0.029$
Right faces		
P1	$F=2.5$, $P=0.090$ New versus standard: $t=0.1$, $P>0.1$ Known versus standard: $t=2.5$, $P=0.042$ New versus known: $t=-1.7$, $P>0.1$	$F=0.5$, $P>0.1$
N290	$F=1.5$, $P>0.1$	$F=0.6$, $P>0.1$
P400	$F=0.1$, $P>0.1$	$F=0.2$, $P>0.1$

The effect of face condition was tested using separate ANOVAs for different ERP components (P1, N290 and P400 responses) and for faces presented in the left and right hemifield. The main effects of the experimental conditions are reported before post hoc Student's *t*-test analyses between conditions taken two by two. *P* values are corrected for multiple comparisons using the FDR approach.

and a longer time to be discriminated, whereas the fast presentation outside the fovea in our paradigm might have favoured a rapid configural analysis done by the right hemisphere[53]. The left- and right-hemifield faces were never directly in competition but were successively presented with a random delay of 550–950 ms. In adults, this delay would be sufficient to reallocate attention from one side to the other, but this probably did not occur in infants, because of their difficulties with rapidly disengaging and reengaging their attention. It may have amplified the spontaneous advantage of the left hemifield.

The N290 amplitude increased with age in response to new faces compared to standard faces, whereas the P400 amplitude showed the opposite effect. This pattern suggests an acceleration of the discrimination response shifting from the P400 to the N290 time-range, and supports the hypothesis that both components are precursors of the adult face-specific N170 component[28]. This acceleration is probably related to the more refined representations of the faces of the infant's environment and of their distinctiveness[21–24,82]. It is noteworthy that the P1 for central stimuli reaches the adult values around 12 weeks of age (Fig. 2c), at the same time infants start to become sensitive to second-order relations[83,84]. This better sensory encoding certainly might help infants perceive more subtle differences.

It has previously been reported[13] that visual input to the right hemisphere during the first postnatal months was necessary for adults to perceive second-order relations: adults with an early left cataract were unable to perceive a change in the spacing between both eyes as well as between the eyes and the mouth in successive pictures of faces, in contrast to adults with an early right cataract. However, they were able to perceive changes in the contours of the face or internal facial features (eyes and mouth) similarly to normal participants. Combined with our results in which only the right hemisphere benefited from a discrimination improvement during the first semester of life; these findings might point to a genuine left-hemispheric difficulty in processing these relations in a face space and therefore to a different microstructural organization of the left and right fusiform regions, probably of genetic origins with a critical window of learning for the right fusiform face area. Within the fusiform gyrus, four regions have been described[85] that are cyto-architectonically dissociable and associated with specific functional domains. Among them, FG2 and FG4 comprise face and word specific areas[85]. As the MRI signal is sensitive not only to water, but also to iron and myelin, quantitative MRI can provide markers for maturation of the grey matter[5]. The maturational timing of these regions and of the neighbouring areas might reveal the microstructural differences that may underlie this functional asymmetry.

Finally, we investigated the efficiency of the inter-hemispheric transfer of visual information. Right-lateralized faces were not discriminated by the left hemisphere. Does this result imply that infants do not process faces presented in their right visual hemifield at all? If this was the case, the right hemifield standard face should have been processed as a new face by the right hemisphere when occasionally presented in the left hemifield (known-deviant condition); however this effect was not present in our study. On the contrary, we observed no difference between the left and right hemifield standard faces regardless of presentation side or cluster, revealing that the transfer of information of facial features was successful when a face was repeated. One could oppose this interpretation by suggesting that the infant may have shifted their gaze to the right hemifield and seen the standard face on this side; however such occurrences, if any, were rare given our visual controls and are likely to be just as rare as the new-face condition. Therefore, without inter-hemispheric transfer, the known-face should have elicited a similar response as to a new face. However, if the inter-hemispheric transfer had been fully efficient, the new face perceived by the left hemisphere should have been transferred to the competent right hemisphere to be discriminated. But we found no significant difference between conditions for the ipsilateral cluster, even at a later time-window for faces presented in the right hemifield. The long IHTT in our group, relative to adults, may have hindered a correct processing of a rare image, whereas the repeated image may have progressively succeeded in obtaining a robust representation in the right hemisphere. Inter-hemispheric transfer is therefore imperfect at this age and may remain so until the end of the second year of life, thereby explaining the behavioural results. Indeed, the cognitive tasks used in two previous behavioural studies investigating trans-callosal transfer were complex: one was based on similarity judgment between two visual items presented simultaneously in the two hemifields[59], and the second on the number of trials needed to learn to discriminate two visual items once the other hemisphere has already learned to discriminate them[51].

Conclusion

Exploiting multimodal imaging in infants, we have demonstrated that lateralized brain processes are not a property of the adult human brain but are observed from the first postnatal weeks onwards, probably because of structural specificities in the genetically specified left–right hemisphere architecture. We have also highlighted that efficient transfer of visual information between hemispheres emerges before 6 months of age, but this transfer is still not fully efficient at this age and probably continues to improve over the course of several months, considering the extended maturation of the corpus callosum. Because our goal was to assess

the functional improvements in relation with structural development, our age range extends over the first postnatal semester and we used the wide variation in the P1 latency. The N290 and P400 latencies are probably also accelerating, introducing inter-subject variability and possibly impinging upon statistical comparisons between conditions. Further studies should examine responses to right-hemifield faces in a more homogeneous group but also at a later age in order to understand how the left hemisphere, and its abilities in featural analyses[52], becomes integrated in the face network. Identifying the anatomo-functional substrates of early visual development is crucial to understanding possible deviations from this normal trajectory and long-term effects of early damage to the visual system.

Methods

We report results obtained in two groups. The first group of infants was studied with both EEG and diffusion MRI to study the functional maturation of visual responses for lateralized stimuli in relation to the structural maturation of white-matter pathways. The second group of infants was tested only with EEG to complete our initial analyses on face discrimination using lateralized stimuli and also to study responses for central faces.

Subjects. The first group consisted of 24 healthy full-term infants aged between 5.8 and 22.4 weeks (mean 14 ± 5.9 weeks, 11 girls). They were first scanned with MRI and then underwent EEG recordings within a week. Two infants had artifacted MRI images, three were not tested with EEG because their parents were unable to return in the predetermined period, and four were rejected due to excessive movement during EEG. Therefore, 22 infants were included in the structural analyses (mean age: 13.8 ± 4.2 weeks), 15 infants in the ERP analyses (mean age: 15 ± 4.1 weeks) and 13 infants had good MRI and EEG data to analyse the correlations between DTI parameters and ERP latencies (mean age: 14 ± 4.3 weeks).

The second group of 25 healthy full-term infants (from 5.6 to 23.6 weeks old, mean age: 13.9 ± 5 weeks, 14 girls) was only tested with EEG. Twelve additional infants were excluded due to insufficient data quality. These 25 infants were merged with the 15 infants described above for a total of 40 infants for whom we studied electrophysiological responses to lateralized face presentations. Out of the 25 infants of the second group, 23 were presented with additional centred faces during the experiment.

The study was approved by the ethical committee for biomedical research. All of the infants' parents were informed about the content of the experiment as well as its goals and gave written informed consent before starting the experiment.

MRI acquisition and post-processing of diffusion images. Acquisitions were performed during spontaneous sleep in a 3T MRI system (Tim Trio, Siemens Healthcare), equipped with a whole-body gradient (40 mT m^{-1}, 200 T m^{-1} s^{-1}) and a 32-channel head coil. T2-weighted (T2w) images were acquired in infants using a 2D turbo spin echo sequence (spatial resolution = 1 × 1 × 1.1 mm^3)[86]. A diffusion-weighted spin-echo EPI sequence was used with 30 orientations of the diffusion gradients applied with $b = 700$ s mm^{-2}. Fifty interleaved axial slices covering the whole brain were acquired with a 1.8-mm isotropic spatial resolution, leading to a total acquisition time of 5 min and 40 s, which is reasonably short for unsedated infants[7].

After correction for motion artifacts with Connectomist software[87,88], probabilistic tractography was performed based on a two-crossing-fibre diffusion model over individual brain masks with FSL software[89]. Using individual seed regions, several tracts were dissected: left and right optic radiations and visual callosal fibres from the visual network as well as acoustic radiations and auditory callosal fibres from the auditory network for comparative purposes. Seeds were localized at the level of lateral geniculate nucleus and occipital regions for optic radiations, and at the level of medial geniculate nucleus and auditory regions for accoustic radiations. Seeds for callosal fibres were located in left and right primary visual/auditory areas and fibres connecting these primary areas should pass through the corpus callosum splenium. Following the estimation of the diffusion tensor, DTI maps (fractional anisotropy, mean $<D>$, transverse $\lambda_{\perp}$ and longitudinal $\lambda_{||}$ diffusivities) were computed for each subject. An averaged parameter X was calculated for each tract by taking into account fibre density on the tract probability map[90]:

$$\overline{X} = \frac{\sum^{i} \mathrm{Pr}_i \times X_i}{\sum^{i} \mathrm{Pr}_i}$$

where i denotes the tract voxels, Pr_i is the fibre density at voxel i, and X_i is the value of the DTI parameter at voxel i. For white matter, DTI parameters are affected by axonal organization, compactness and myelination. We focused on transverse diffusivity, which has been shown to be the best DTI marker of myelination[6,64,65].

EEG protocol. *Experimental paradigm.* Coloured front faces of four female and four male adults with neutral expressions were used as visual stimuli. Six of these images were used for lateralized presentation and two for centred presentation. The image presentation was driven by E-Prime (Psycho-logical Software Products)(Fig. 1).

Lateralized paradigm. The infants' eyes were attracted to the centre of the screen by a rotating coloured bull's-eye that remained at the centre of the screen during the whole experiment. Two streams of face images were presented on the left and right side of the rotating bull's eye (Fig. 1b,c). The centre of the image was at around 7.5 degrees of eccentricity from the infants' centre of view, its inner/outer edges at about 3.1/12.5 degrees of eccentricity for an infant sitting at about 60 cm from the screen. Each image was presented for 250 ms. The left and right images were presented asynchronously in an alternating fashion with a variable delay between images (550 to 950 ms post-offset of the image with a 50-ms step) to avoid anticipatory looks to the sides. Each stream included three types of images: a side-assigned face image (standard), a novel face (new-deviant), or the face commonly assigned to the other side (known-deviant). Inside a block, the faces were either all female or all male. Two similar paradigms but with different trial organizations were used for the two groups of infants.

The first group consisted of 15 infants. To familiarize infants with the experimental paradigm and for them to learn the face-side assignment, 8 standard trials with side-assigned faces were first presented on each side (habituation phase). Then in a test phase, 54 trials were presented on each side, with a succession of 18 three-trial structures: two standard trials and the third trial randomly chosen among either a standard, new- or known-deviant condition (Fig. 1e). Over the 54 trials, 42 (77.8 %) were therefore standard trials, and 6 (11.1%) were new- or known-deviant trials. Each block included 124 trials (2 sides × (8 habituation + 54 test) trials), out of which 80.6 % were standard, 9.7 % new-deviant and 9.7 % known-deviant. The whole experiment comprised four blocks alternating between female and male faces (9 min).

The second group consisted of 25 infants. In the first group, the side of the first block image was not counterbalanced across infants, implying that the critical third image of the three-trial structure (standard versus new- versus known-deviant faces) was always presented on the left side before the right side. In the second group, we controlled for trial order, such that: (1) Deviant trials were preceded by a similar number of standard trials on both left and right sides. (2) No two successive deviant faces at the same or opposite sides were allowed. Infants were presented with 4 blocks of 80 trials on each side (60 standard, 10 new-deviant, 10 known-deviant). As for the first group, 8 standard trials were presented at the beginning of each block in each hemifield, leading to 176 trials per block (2 sides × (8 habituation + 80 test) trials), out of which 77.3 % were standard, 11.4 % new-deviant and 11.4 % known-deviant.

Central paradigm (23 infants). We took advantage of this second group to test infants' responses to centred stimuli. Four additional blocks of 30 trials (two images with female and two with male faces) were presented after the blocks with lateralized stimuli. One female and one male face, not used during the lateralized paradigm, were presented at the centre of the screen for 250 ms, spaced by a random interval of 250–550 ms during which the coloured bull's eye was presented (Fig. 1a). The total duration of the second experiment (lateralized + centred paradigms) was at most 15 min.

EEG data acquisition. An EEG recording net comprising 128 electrodes (EGI) with a reference on the vertex was placed on the infants' heads relative to anatomical markers. Infants were seated on their parents' laps in front of the screen in a shielded EEG room. Music was continuously played behind the screen to attract the infants' attention toward the screen. If an infant was distracted, the experiment was briefly interrupted and the experimenter focused her/his attention back toward the screen. If it was not possible, the experiment was prematurely terminated. A camera placed above the screen recorded the infants' position and looking direction throughout the experiment. EEG was continuously digitized at a sampling rate of 250 Hz during the whole experiment (net amp 200 system EGI).

EEG processing and ERP analyses. *EEG pre-processing.* EEG recordings were band-pass filtered between 0.5 and 20 Hz on the EGI recording station, then exported to be processed using MATLAB toolboxes: EEGLAB[91] and Brainstorm[92]. The signal was segmented into epochs of 1,700 ms (−200 to +1,500 ms relative to the onset of each face presentation). Channels contaminated by movement or eye artifacts were automatically rejected on a trial-by-trial basis based on amplitude variations inside an epoch: each channel epoch was rejected when the fast average amplitude exceeded 250 μV, or when deviation between fast and slow running averages exceeded 150 μV. Electrodes were rejected if they were marked as bad in more than 70% of the epochs, and trials were rejected if more than 50% of the electrodes were marked bad. Recordings were then re-referenced by subtracting the average activity of all channels over the brain to obtain average-reference recordings, then baseline-corrected by the 200 ms preceding the onset of the image presentation. On average, we obtained 171/170 correct trials, respectively, for the left/right hemifield faces in the first group of infants, and 72/71/37 for

the left/right/centre location in the second group. For each infant, trials were first averaged by stimulus side (that is, left/right/centre) in order to evaluate the early visual ERP responses (that is, P1). Then trials were averaged by condition (standard faces, new- or known-deviant faces in the left and right hemifield) to study face discrimination.

Early visual perception. **P1 latencies.** For left/right hemifield presentation, we evaluated the latency of the contralateral and ipsilateral P1 across the two groups (15 + 25 = 40 infants). For the grand average topography, we identified two symmetrical clusters of five electrodes around O1 and O2 for which early visual responses were observed independent of the infants' ages. We averaged the time-series across the electrode clusters in each infant and measured the latencies of the following components (Fig. 2b): P1 as the first positive peak in the hemisphere contralateral to the image, and P1 ipsi as the first positive peak appearing after P1 in the hemisphere ipsilateral to the stimulation. The inter-hemispheric transfer time (IHTT) was defined as the latency difference between these two peaks ($\mathrm{IHTT} = \mathrm{Latency}_{\mathrm{P1_{Ipsi}}} - \mathrm{Latency}_{\mathrm{P1}}$). For central faces, P1 latency was identified in each infant as the first positive peak over a cluster of 6 mid-occipital electrodes surrounding Oz (Fig. 2a).

Effect of age on P1 latencies and transverse diffusivity. We first assessed the effect of age on functional and structural measurements, that is, contralateral P1, IHTT and central P1 on the one hand; and on transverse diffusivity in optic/auditory radiations and visual/auditory callosal fibres on the other hand. To evaluate domain-specific maturational patterns beyond a general effect of age, we computed partial correlations (controlling for age) between transverse diffusivity measurements for the 4 pairs of tracts. We used a false-discovery rate (FDR) approach to correct for the number of comparisons. Finally, we tested hemispheric asymmetries in the optic and acoustic radiations with paired *t*-tests on the transverse diffusivity in the left and right tracts.

Relationships between P1 latencies and tract-specific transverse diffusivity. We proceeded by examining the relationship between functional and structural measurements of maturation. Because ERP latencies depend on the distance the neural signal has to travel in addition to the myelination of pathways, we computed conduction speeds of ERP responses (distance / latency) using anatomical distances in the brain. For contralateral P1 latency, we approximated the length of the optic radiations as the distance between the eyes and the occipital poles measured on each individual infant's T2w images as in our previous study[6] and computed the conduction speed of P1 ($\mathrm{Speed_{P1}}$). For inter-hemispheric transfer time, we measured the length of the callosal fibres obtained by tractography and computed the speed of inter-hemispheric transfer ($\mathrm{Speed_{IHTT}}$). To confirm the specificity of these results to the visual domain, we performed the same analysis, but considering the acoustic radiations and auditory callosal fibres as surrogate tracts for $\mathrm{Speed_{P1}}$ and $\mathrm{Speed_{IHTT}}$, respectively. We used FDR approach to correct for the four comparisons.

Discrimination of lateralized presented faces. To study face-discrimination responses, we considered only the standard and deviant trials that were in the same position in the block structure. For the first group for which faces were presented in a three-trial structure, we considered the third face of the structure, which was either a standard, known-deviant or new-deviant face. In the second group to mimic the constraints imposed on deviant trials in the first paradigm, we selected the standard faces following at least two standard faces on the same or opposite side. The numbers of trials considered in each condition was therefore balanced. On average, we obtained 11/10/14 trials per subject for the new-deviant/known-deviant/standard conditions for each side. Epochs were averaged for each condition and side of presentation in each infant. As results were similar in the two groups, the data were merged.

In the literature, two face-specific components, the N290 and the P400 recorded over the lower temporal regions, have been reported in infants[25]. We thus selected two clusters of 10 electrodes in the left and right inferior temporal regions extending from O1/O2 to T5/T6 electrodes on the 10–20 international system (as in ref. [93]). For each experimental condition, we averaged the voltage over these electrodes and over a 100-ms time window centred on each component's peak in each infant. The peaks were determined on the grand average from merging all conditions and infants. Therefore, we analysed the three visual components (P1, N290 and P400) for the following time windows 150–250 ms for the P1, 300–400 ms for N290 and 450–550 ms for P400 (Fig. 4). The time windows are slightly delayed compared to the classical timing of N290 and P400 components as latencies are delayed for lateralized stimuli relative to central stimuli and also because our infant cohort is younger than those most commonly tested.

The voltage amplitudes were entered in three independent analyses of variance, each comprising three within-subject factors: condition (standard, known-deviant and new-deviant), electrodes (left and right cluster), and side of stimulation (left and right hemifield). We examined two effects of interest in post hoc analyses using paired *t*-tests: (1) Whether the new-deviant condition was significantly different from the standard condition in order to demonstrate face discrimination capabilities. (2) Whether the known-deviant condition was significantly different from the new-deviant condition or from the standard condition in order to evaluate the efficiency of the inter-hemispheric transfer. Finally, we evaluated whether the face-discrimination response was correlated with age using robust regression. We report significant effects with a *P* value below 0.05, once corrected for multiple comparisons using FDR correction.

Life Sciences Reporting Summary. Further information on experimental design is available in the Life Sciences Reporting Summary.

Code availability. The analysis code that supports the findings of this study is available from the corresponding author upon request.

Data availability. The data and analysis code that support the findings of this study are available from the corresponding author upon request.

Received: 27 February 2017; Accepted: 19 October 2017;
Published online: 11 December 2017

References

1. Dehaene, S. *Reading in the Brain: The New Science of How We Read* (Penguin, New York, NY, 2009).
2. Rakic, P. Specification of cerebral cortical areas. *Science* **241**, 170–176 (1988).
3. de Schonen, S. & Mathivet, E. First come, first served: a scenario about the development of hemispheric specialization in face recognition during infancy. *Curr. Psychol. Cogn.* **9**, 3–44 (1989).
4. Dehaene-Lambertz, G. & Spelke, E. S. The infancy of the human brain. *Neuron* **88**, 93–109 (2015).
5. Leroy, F. et al. Early maturation of the linguistic dorsal pathway in human infants. *J. Neurosci.* **31**, 1500–1506 (2011).
6. Dubois, J. et al. Microstructural correlates of infant functional development: example of the visual pathways. *J. Neurosci.* **28**, 1943–1948 (2008).
7. Dubois, J. et al. Exploring the early organization and maturation of linguistic pathways in the human infant brain. *Cereb. Cortex* **26**, 2283–2298 (2016).
8. Johnson, M. H. Functional brain development in humans. *Nat. Rev. Neurosci.* **2**, 475–483 (2001).
9. Saygin, Z. M. et al. Connectivity precedes function in the development of the visual word form area. *Nat. Neurosci.* **19**, 1250–1255 (2016).
10. Dundas, E. M., Plaut, D. C. & Behrmann, M. The joint development of hemispheric lateralization for words and faces. *J. Exp. Psychol. Gen.* **142**, 348–358 (2013).
11. Monzalvo, K., Fluss, J., Billard, C., Dehaene, S. & Dehaene-Lambertz, G. Cortical networks for vision and language in dyslexic and normal children of variable socio-economic status. *Neuroimage* **61**, 258–274 (2012).
12. Dehaene, S. et al. How learning to read changes the cortical networks for vision and language. *Science* **330**, 1359–1364 (2010).
13. Le Grand, R., Mondloch, C. J., Maurer, D. & Brent, H. P. Expert face processing requires visual input to the right hemisphere during infancy. *Nat. Neurosci.* **6**, 1108–1112 (2003).
14. Acerra, F., Burnod, Y. & de Schonen, S. Modelling aspects of face processing in early infancy. *Dev. Sci.* **5**, 98–117 (2002).
15. Gauthier, I. & Nelson, C. A. The development of face expertise. *Curr. Opin. Neurobiol.* **11**, 219–224 (2001).
16. Morton, J. & Johnson, M. H. CONSPEC and CONLERN: a two-process theory of infant face recognition. *Psychol. Rev.* **98**, 164–181 (1991).
17. Bushnell, I. W. R., Sai, F. & Mullin, J. T. Neonatal recognition of the mother's face. *Br. J. Dev. Psychol.* **7**, 3–15 (1989).
18. Pascalis, O., de Schonen, S., Morton, J., Deruelle, C. & Fabre-Grenet, M. Mother's face recognition by neonates: a replication and an extension. *Infant Behav. Devel.* **18**, 79–85 (1995).
19. Turati, C., Bulf, H. & Simion, F. Newborns' face recognition over changes in viewpoint. *Cognition* **106**, 1300–1321 (2008).
20. Cohen, L. B. & Strauss, M. S. Concept acquisition in the human infant. *Child Dev.* **50**, 419–424 (1979).
21. Kelly, D. J. et al. Three-month-olds, but not newborns, prefer own-race faces. *Dev. Sci.* **8**, F31–F36 (2005).
22. Quinn, P. C. et al. Infant preference for female faces occurs for same- but not other-race faces. *J. Neuropsychol.* **2**, 15–26 (2008).
23. Quinn, P. C., Yahr, J., Kuhn, A., Slater, A. M. & Pascalils, O. Representation of the gender of human faces by infants: a preference for female. *Perception* **31**, 1109–1121 (2002).
24. Righi, G., Westerlund, A., Congdon, E. L., Troller-Renfree, S. & Nelson, C. A. Infants' experience-dependent processing of male and female faces: insights from eye tracking and event-related potentials. *Dev. Cogn. Neurosci.* **8**, 144–152 (2014).
25. de Haan, M., Pascalis, O. & Johnson, M. H. Specialization of neural mechanisms underlying face recognition in human infants. *J. Cogn. Neurosci.* **14**, 199–209 (2002).
26. Gliga, T. & Dehaene-Lambertz, G. Structural encoding of body and face in human infants and adults. *J. Cogn. Neurosci.* **17**, 1328–1340 (2005).

27. Gliga, T. & Dehaene-Lambertz, G. Development of a view-invariant representation of the human head. *Cognition* **102**, 261–288 (2007).
28. Halit, H., de Haan, M. & Johnson, M. H. Cortical specialisation for face processing: face-sensitive event-related potential components in 3- and 12-month-old infants. *Neuroimage* **19**, 1180–1193 (2003).
29. Key, A. P. F. & Stone, W. L. Processing of novel and familiar faces in infants at average and high risk for autism. *Dev. Cogn. Neurosci.* **2**, 244–255 (2012).
30. Peykarjou, S., Pauen, S. & Hoehl, S. 9-month-old infants recognize individual unfamiliar faces in a rapid repetition ERP paradigm. *Infancy* **21**, 288–311 (2016).
31. Scott, L. S. & Nelson, C. A. Featural and configural face processing in adults and infants: a behavioral and electrophysiological investigation. *Perception* **35**, 1107–1128 (2006).
32. Scott, L. S., Shannon, R. W. & Nelson, C. A. Neural correlates of human and monkey face processing in 9-month-old infants. *Infancy* **10**, 171–186 (2006).
33. de Heering, A. & Rossion, B. Rapid categorization of natural face images in the infant right hemisphere. *eLife* **4**, e06564 (2015).
34. Rossion, B., Torfs, K., Jacques, C. & Liu-Shuang, J. Fast periodic presentation of natural images reveals a robust face-selective electrophysiological response in the human brain. *J. Vis.* **15**, 1–18 (2015).
35. Honda, Y. et al. How do infants perceive scrambled face? A near-infrared spectroscopic study. *Brain Res.* **1308**, 137–146 (2010).
36. Nakato, E. et al. I know this face: neural activity during mother's face perception in 7- to 8-month-old infants as investigated by near-infrared spectroscopy. *Early Hum. Dev.* **87**, 1–7 (2011).
37. Otsuka, Y. et al. Neural activation to upright and inverted faces in infants measured by near infrared spectroscopy. *Neuroimage* **34**, 399–406 (2007).
38. Nakato, E. et al. When do infants differentiate profile face from frontal face? A near-infrared spectroscopic study. *Human Brain Mapp.* **30**, 462–472 (2009).
39. Tzourio-Mazoyer, N. et al. Neural correlates of woman face processing by 2-month-old infants. *Neuroimage* **15**, 454–461 (2002).
40. Deen, B. et al. Organization of high-level visual cortex in human infants. *Nat. Commun.* **8**, 13995 (2017).
41. Scherf, K. S., Behrmann, M., Humphreys, K. & Luna, B. Visual category-selectivity for faces, places and objects emerges along different developmental trajectories. *Dev. Sci.* **10**, F15–F30 (2007).
42. Cantlon, J. F., Pinel, P., Dehaene, S. & Pelphrey, K. A. Cortical representations of symbols, objects, and faces are pruned back during early childhood. *Cereb. Cortex* **21**, 191–199 (2011).
43. Gathers, A. D., Bhatt, R., Corbly, C. R., Farley, A. B. & Joseph, J. E. Developmental shifts in cortical loci for face and object recognition. *Neuroreport* **15**, 1549–1553 (2004).
44. Golarai, G. et al. Differential development of high-level visual cortex correlates with category-specific recognition memory. *Nat. Neurosci.* **10**, 512–522 (2007).
45. Peelen, M. V., Glaser, B., Vuilleumier, P. & Eliez, S. Differential development of selectivity for faces and bodies in the fusiform gyrus. *Dev. Sci.* **12**, F16–F25 (2009).
46. Gomez, J. et al. Microstructural proliferation in human cortex is coupled with the development of face processing. *Science* **355**, 68–71 (2017).
47. Rizzolatti, G., Umilta, C. & Berlucchi, G. Opposite superiorities of the right and left cerebral hemispheres in discriminative reaction time to physiognomical and alphabetical material. *Brain* **94**, 431–442 (1971).
48. Cohen, L. et al. The visual word form area: spatial and temporal characterization of an initial stage of reading in normal subjects and posterior split-brain patients. *Brain* **123**, 291–307 (2000).
49. Verosky, S. C. & Turk-Browne, N. B. Representations of facial identity in the left hemisphere require right hemisphere processing. *J. Cogn. Neurosci.* **24**, 1006–1017 (2012).
50. de Schonen, S., de Diaz, M. G. D. & Mathivet, E. in *Aspects of Face Processing* (eds Ellis, H. D., Jeeves, M., Newcombe, F. & Young, A.) 199–209 (Springer Amsterdam, 1986).
51. de Schonen, S. & Mathivet, E. Hemispheric asymmetry in a face discrimination task in infants. *Child Dev.* **61**, 1192–1205 (1990).
52. Deruelle, C. & de Schonen, S. Do the right and left hemispheres attend to the same visuospatial information within a face in infancy? *Dev. Neuropsychol.* **14**, 535–554 (1998).
53. Kostovic, I. & Jovanov-Milosevic, N. The development of cerebral connections during the first 20–45 weeks' gestation. *Semin. Fetal Neonatal Med.* **11**, 415–422 (2006).
54. Brody, B. A., Kinney, H. C., Kloman, A. S. & Gilles, F. H. Sequence of central nervous system myelination in human infancy. I. An autopsy study of myelination. *J. Neuropathol. Exp. Neurol.* **46**, 283–301 (1987).
55. Yakovlev P. L. & Lecours, A. R. in *Regional Development of the Brain in Early Life* (ed. Minkowski, A.) 3–69 (Blackwell, Oxford, 1967).
56. Nakagawa, H. et al. Normal myelination of anatomic nerve fiber bundles: MR analysis. *AJNR Am. J. Neuroradiol.* **19**, 1129–1136 (1998).
57. Levitan, S. & Reggia, J. A. A computational model of lateralization and asymmetries in cortical maps. *Neural Comput.* **12**, 2037–2062 (2000).
58. de Schonen, S. & Bry, I. Interhemispheric communication of visual learning: a developmental study in 3–6-month old infants. *Neuropsychologia* **25**, 601–612 (1987).
59. Liégeois, F., Bentejac, L. & de Schonen, S. When does inter-hemispheric integration of visual events emerge in infancy? A developmental study on 19- to 28-month-old infants. *Neuropsychologia* **38**, 1382–1389 (2000).
60. Sann, C. & Streri, A. Perception of object shape and texture in human newborns: evidence from cross-modal transfer tasks. *Dev. Sci.* **10**, 399–410 (2007).
61. Flechsig, P. E. *Anatomie des menschlichen Gehirns und Rückenmarks auf myelogenetischer Grundlage* Vol. 1 (G. Thieme, Leipzig, 1920).
62. Dubois, J. et al. The early development of brain white matter: a review of imaging studies in fetuses, newborns and infants. *Neuroscience* **276**, 48–71 (2014).
63. Neil, J., Miller, J., Mukherjee, P. & Huppi, P. S. Diffusion tensor imaging of normal and injured developing human brain—a technical review. *NMR Biomed.* **15**, 543–552 (2002).
64. Song, S. K. et al. Diffusion tensor imaging detects and differentiates axon and myelin degeneration in mouse optic nerve after retinal ischemia. *Neuroimage* **20**, 1714–1722 (2003).
65. Song, S. K. et al. Demyelination increases radial diffusivity in corpus callosum of mouse brain. *Neuroimage* **26**, 132–140 (2005).
66. McCulloch, D. L., Orbach, H. & Skarf, B. Maturation of the pattern-reversal VEP in human infants: a theoretical framework. *Vision Res.* **39**, 3673–3680 (1999).
67. Westerhausen, R. et al. Interhemispheric transfer time and structural properties of the corpus callosum. *Neurosci. Lett.* **409**, 140–145 (2006).
68. Whitford, T. J. et al. Predicting inter-hemispheric transfer time from the diffusion properties of the corpus callosum in healthy individuals and schizophrenia patients: a combined ERP and DTI study. *Neuroimage* **54**, 2318–2329 (2011).
69. Horowitz, A. et al. In vivo correlation between axon diameter and conduction velocity in the human brain. *Brain Struct. Funct.* **220**, 1777–1788 (2015).
70. Akaike, H. in *International Encyclopedia of Statistical Science* (ed. Lovric, M.) 25 (Springer, Berlin, 2011).
71. Lippe, S., Roy, M.-S., Perchet, C. & Lassonde, M. Electrophysiological markers of visuocortical development. *Cereb. Cortex* **17**, 100–107 (2007).
72. Allen, D., Tyler, C. W. & Norcia, A. M. Development of grating acuity and contrast sensitivity in the central and peripheral visual field of the human infant. *Vision Res.* **36**, 1945–1953 (1996).
73. Tachibanaki, S., Arinobu, D., Shimauchi-Matsukawa, Y., Tsushima, S. & Kawamura, S. Highly effective phosphorylation by G protein-coupled receptor kinase 7 of light-activated visual pigment in cones. *Proc. Natl Acad. Sci. USA* **102**, 9329–9334 (2005).
74. Saron, C. D. & Davidson, R. J. Visual evoked potential measures of interhemispheric transfer time in humans. *Behav. Neurosci.* **103**, 1115–1138 (1989).
75. Honda, Y., Watanabe, S., Nakamura, M., Miki, K. & Kakigi, R. Interhemispheric difference for upright and inverted face perception in humans: an event-related potential study. *Brain Topogr.* **20**, 31–39 (2007).
76. Ringo, J. L., Doty, R. W., Demeter, S. & Simard, P. Y. Time is of the essence: a conjecture that hemispheric specialization arises from interhemispheric conduction delay. *Cereb. Cortex* **4**, 331–343 (1994).
77. Kulke, L., Atkinson, J. & Braddick, O. Automatic detection of attention shifts in infancy: eye tracking in the fixation shift paradigm. *PLoS ONE* **10**, e0142505 (2015).
78. Rossion, B. & Caharel, S. ERP evidence for the speed of face categorization in the human brain: disentangling the contribution of low-level visual cues from face perception. *Vision Res.* **51**, 1297–1311 (2011).
79. Yovel, G., Tambini, A. & Brandman, T. The asymmetry of the fusiform face area is a stable individual characteristic that underlies the left-visual-field superiority for faces. *Neuropsychologia* **46**, 3061–3068 (2008).
80. Kobayashi, M., Cassia, V. M., Kanazawa, S., Yamaguchi, M. K. & Kakigi, R. Perceptual narrowing towards adult faces is a cross-cultural phenomenon in infancy a behavioral and near-infrared spectroscopy study with Japanese infants. *Dev. Sci.* http://dx.doi.org/10.1111/desc.12498 (2016).
81. Kobayashi, M. et al. Do infants represent the face in a viewpoint-invariant manner? Neural adaptation study as measured by near-infrared spectroscopy. *Front. Hum. Neurosci.* **5**, 153 (2011).
82. Sangrigoli, S. & de Schonen, S. Recognition of own-race and other-race faces by three-month-old infants. *J. Child Psychol. Psychiatry* **45**, 1219–1227 (2004).
83. Bhatt, R. S., Bertin, E., Hayden, A. & Reed, A. Face processing in infancy: developmental changes in the use of different kinds of relational information. *Child Dev.* **76**, 169–181 (2005).
84. Bhatt, R. S., Bertin, E., Hayden, A. & Reed, A. Face processing in infancy developmental changes in the use of different kinds of relational information. *Child Dev.* **76**, 169–181 (2005).

85. Weiner, K. S. et al. The cytoarchitecture of domain-specific regions in human high-level visual cortex. *Cereb. Cortex* **27**, 146–161 (2016).
86. Kabdebon, C. et al. Anatomical correlations of the international 10–20 sensor placement system in infants. *Neuroimage* **99**, 342–356 (2014).
87. Dubois, J. et al. Correction strategy for diffusion-weighted images corrupted with motion: application to the DTI evaluation of infants' white matter. *Magn. Reson. Imaging* **32**, 981–992 (2014).
88. Duclap, D. et al. Connectomist-2.0: a novel diffusion analysis toolbox for BrainVISA. in *29th ESMRMB* (2012).
89. Behrens, T. E., Berg, H. J., Jbabdi, S., Rushworth, M. F. & Woolrich, M. W. Probabilistic diffusion tractography with multiple fibre orientations: What can we gain? *Neuroimage* **34**, 144–155 (2007).
90. Hua, K. et al. Tract probability maps in stereotaxic spaces: analyses of white matter anatomy and tract-specific quantification. *Neuroimage* **39**, 336–347 (2008).
91. Delorme, A. & Makeig, S. EEGLAB: an open source toolbox for analysis of single-trial EEG dynamics including independent component analysis. *J. Neurosci. Methods* **134**, 9–21 (2004).
92. Tadel, F., Baillet, S., Mosher, J. C., Pantazis, D. & Leahy, R. M. Brainstorm: a user-friendly application for MEG/EEG analysis. *Comput. Intell. Neurosci.* **2011**, 879716 (2011).
93. Kouider, S. et al. A neural marker of perceptual consciousness in infants. *Science* **340**, 376–380 (2013).

Acknowledgements

This research was supported by grants from the Fondation de France and the Fyssen Foundation. The funders had no role in study design, data collection and analysis, decision to publish, or preparation of the manuscript. We thank all the infants and their parents who participated in this study as well as G. Santoro and the medical team of UNIACT at Neurospin, who helped to carry out the experiments; C. Kabdebon, P. Barttfeld, J. Lebenberg and F. Leroy for their help with the EEG and MRI analyses; and E. Moulton for proofreading the text. We thank our colleagues for providing their pictures to be used as stimuli in our paradigm.

Author contributions

All authors contributed to data collection, analysis, interpretation and drafting of the Article. J.D. and G.D.-L. designed the experiments.

Competing interests

The authors declare no competing financial interests.

Additional information

Supplementary information is available for this paper at https://doi.org/10.1038/s41562-017-0249-4.

Reprints and permissions information is available at www.nature.com/reprints.

Correspondence and requests for materials should be addressed to G.D.

Publisher's note: Springer Nature remains neutral with regard to jurisdictional claims in published maps and institutional affiliations.

nature research

Corresponding author(s): Ghislaine Dehaene-Lambertz

☐ Initial submission ☐ Revised version ☒ Final submission

Life Sciences Reporting Summary

Nature Research wishes to improve the reproducibility of the work that we publish. This form is intended for publication with all accepted life science papers and provides structure for consistency and transparency in reporting. Every life science submission will use this form; some list items might not apply to an individual manuscript, but all fields must be completed for clarity.

For further information on the points included in this form, see Reporting Life Sciences Research. For further information on Nature Research policies, including our data availability policy, see Authors & Referees and the Editorial Policy Checklist.

Experimental design

1. Sample size

Describe how sample size was determined.

A total of 40 and 22 infants were included in the EEG and MRI studies respectively, respecting typical sample size in infant studies . 13 infants had adequate data for both studies, which is fair considering the difficulties of acquiring both types of data in a young population.

2. Data exclusions

Describe any data exclusions.

We excluded ~ 30 infants from the EEG study, because we could not obtain appropriate data in these infants. The exclusion criteria were:
- low tolerance of infants during the experiment and thus insufficient recording time.
- extensive movements during the experiment creating large artefacts in the data
- low number of trials per experimental condition after the preprocessing,
- presence of several saccadic eye movements after checking the recorded videos of the experiment.

We also excluded ~20 infants from MRI study, since no good data could be obtained for them.

3. Replication

Describe whether the experimental findings were reliably reproduced.

The EEG experiment was carried out in two infant groups and the right-hemisphere face discrimination responses were reproduced in both groups.

4. Randomization

Describe how samples/organisms/participants were allocated into experimental groups.

The experiment consisted of intra-subject comparisons and did not require randomization of participants into groups.

5. Blinding

Describe whether the investigators were blinded to group allocation during data collection and/or analysis.

The experiment consisted of intra-subject comparisons and did not require randomization of participants into groups that investigators should have been blinded to.

Note: all studies involving animals and/or human research participants must disclose whether blinding and randomization were used.

6. Statistical parameters

For all figures and tables that use statistical methods, confirm that the following items are present in relevant figure legends (or in the Methods section if additional space is needed).

n/a	Confirmed
☐	☒ The exact sample size (*n*) for each experimental group/condition, given as a discrete number and unit of measurement (animals, litters, cultures, etc.)
☐	☒ A description of how samples were collected, noting whether measurements were taken from distinct samples or whether the same sample was measured repeatedly
☐	☒ A statement indicating how many times each experiment was replicated
☐	☒ The statistical test(s) used and whether they are one- or two-sided (note: only common tests should be described solely by name; more complex techniques should be described in the Methods section)
☐	☒ A description of any assumptions or corrections, such as an adjustment for multiple comparisons
☐	☒ The test results (e.g. *P* values) given as exact values whenever possible and with confidence intervals noted
☐	☒ A clear description of statistics including central tendency (e.g. median, mean) and variation (e.g. standard deviation, interquartile range)
☐	☒ Clearly defined error bars

See the web collection on statistics for biologists for further resources and guidance.

Software

Policy information about availability of computer code

7. Software

Describe the software used to analyze the data in this study.

EEG : Matlab toolboxes (EEGLAB and Brainstorm) and some in-house codes ran under Matlab were used to analyze the EEG data.
MRI: Connectomist software was used for motion artifact corrections and FSL was used for tractography and computing DTI maps.

For manuscripts utilizing custom algorithms or software that are central to the paper but not yet described in the published literature, software must be made available to editors and reviewers upon request. We strongly encourage code deposition in a community repository (e.g. GitHub). *Nature Methods* guidance for providing algorithms and software for publication provides further information on this topic.

Materials and reagents

Policy information about availability of materials

8. Materials availability

Indicate whether there are restrictions on availability of unique materials or if these materials are only available for distribution by a for-profit company.

The data is available upon request.

9. Antibodies

Describe the antibodies used and how they were validated for use in the system under study (i.e. assay and species).

No antibodies were used.

10. Eukaryotic cell lines

a. State the source of each eukaryotic cell line used.

no eukaryotic cell lines were used.

b. Describe the method of cell line authentication used.

no eukaryotic cell lines were used.

c. Report whether the cell lines were tested for mycoplasma contamination.

no eukaryotic cell lines were used.

d. If any of the cell lines used are listed in the database of commonly misidentified cell lines maintained by ICLAC, provide a scientific rationale for their use.

no commonly misidentified cell lines were used.

Animals and human research participants

Policy information about studies involving animals; when reporting animal research, follow the ARRIVE guidelines

11. Description of research animals

Provide details on animals and/or animal-derived materials used in the study.	no animals were used.

Policy information about studies involving human research participants

12. Description of human research participants

Describe the covariate-relevant population characteristics of the human research participants.	40 and 22 healthy full-term infants were included in the EEG and MRI experiments. Age was entered as a covariable. The study was approved by the ethical committee for biomedical research. All of the infants' parents were informed about the content of the experiment as well as its goals and gave written informed consent before starting the experiment.

nature research

Corresponding author(s): Ghislaine Dehaene-Lambertz

☐ Initial submission ☐ Revised version ☒ Final submission

MRI Studies Reporting Summary

Form fields will expand as needed. Please do not leave fields blank.

Experimental design

1. Describe the experimental design.	N/A
2. Specify the number of blocks, trials or experimental units per session and/or subject, and specify the length of each trial or block (if trials are blocked) and interval between trials.	N/A
3. Describe how behavioral performance was measured.	N/A

Acquisition

4. Imaging

a. Specify the type(s) of imaging.	Structural and diffusion MRI
b. Specify the field strength (in Tesla).	3 T
c. Provide the essential sequence imaging parameters.	T2w images were obtained with a 2D turbo spin echo sequence (TSE, TE/TR= 149/4500 ms, 4 concatenations, parallel imaging GRAPPA reduction factor 2). Axial slices were acquired with a spatial resolution of 1x1x1.1 mm (field of view = 192mm; acquisition matrix=192 ×192, no interpolation at reconstruction; slice thickness = 1.1 mm; 92 slices). For diffusion MRI, spin echo EPI sequence was used (TE/TR = 72/10000 ms). 50 interleaved axial slices were acquired with a 1.8mm isotropic spatial resolution (field of view= 230 mm, matrix = 128 × 128). To minimize specific absorption rate (SAR) and noise exposure, we used radio-frequency impulsions with “no SAR”, and the “whisper” gradients mode in these sequences.
d. For diffusion MRI, provide full details of imaging parameters.	30 orientations of the diffusion gradients were applied with b=700s.mm-2.

5. State area of acquisition.	whole brain

Preprocessing

6. Describe the software used for preprocessing.	Pre-processings, notably correction of motion artifacts, were performed with Connectomist software (PTK software, NeuroSpin; see Dubois et al, Magnetic Resonance Imaging 2014). Tractography and quantification of DTI maps was performed using FSL (Behrens et al., 2007).

7. Normalization

a. If data were normalized/standardized, describe the approach(es).	No normalization was used
b. Describe the template used for normalization/ transformation.	No normalization was used
8. Describe your procedure for artifact and structured noise removal.	Motion artifacts were corrected with Connectomist software (PTK software, NeuroSpin; see Dubois et al, Magnetic Resonance Imaging 2014)

9. Define your software and/or method and criteria for volume censoring, and state the extent of such censoring.	N/A

Statistical modeling & inference

10. Define your model type and settings.	N/A
11. Specify the precise effect tested.	N/A
12. Analysis	
a. Specify whether analysis is whole brain or ROI-based.	DTI maps were computed over the whole brain. Quantification of DTI parameters was restricted to the white matter pathways of interest that were reconstructed with tractography.
b. If ROI-based, describe how anatomical locations were determined.	Bundles of interest were reconstructed with tractography, for which seeds were drawn manually in each infant by one experimenter (PA).
13. State the statistic type for inference. (See Eklund et al. 2016.)	Age-related changes in DTI parameters were assessed using Pearson correlations, and maturation relationships across bundles, beyond age effects, were assessed using partial correlations.
14. Describe the type of correction and how it is obtained for multiple comparisons.	FDR approach was used to correct for the number of correlations and partial correlations that were evaluated.
15. Connectivity	
a. For functional and/or effective connectivity, report the measures of dependence used and the model details.	N/A
b. For graph analysis, report the dependent variable and functional connectivity measure.	N/A
16. For multivariate modeling and predictive analysis, specify independent variables, features extraction and dimension reduction, model, training and evaluation metrics.	N/A